CHAPTER IV
RESULTS AND DISCUSSION

4.1 Effect of Catalysts on Hydrogen Desorption in Li-N-H Systems

4.1.1 Mixed by Mortar and Pestle

A mixture of $LiNH_2$ and LiH (1:1 mol ratio) was added with 1 mol% TiO_2 or Fe and mixed by using mortar and pestle for 15 min. Effects of the catalysts on hydrogen desorption are shown in Figure 4.1. The amounts of released hydrogen from all samples are relatively the same, about 0.4 – 0.5 wt% at 200°C. In addition, either catalyst barely affects the hydrogen desorption kinetics.

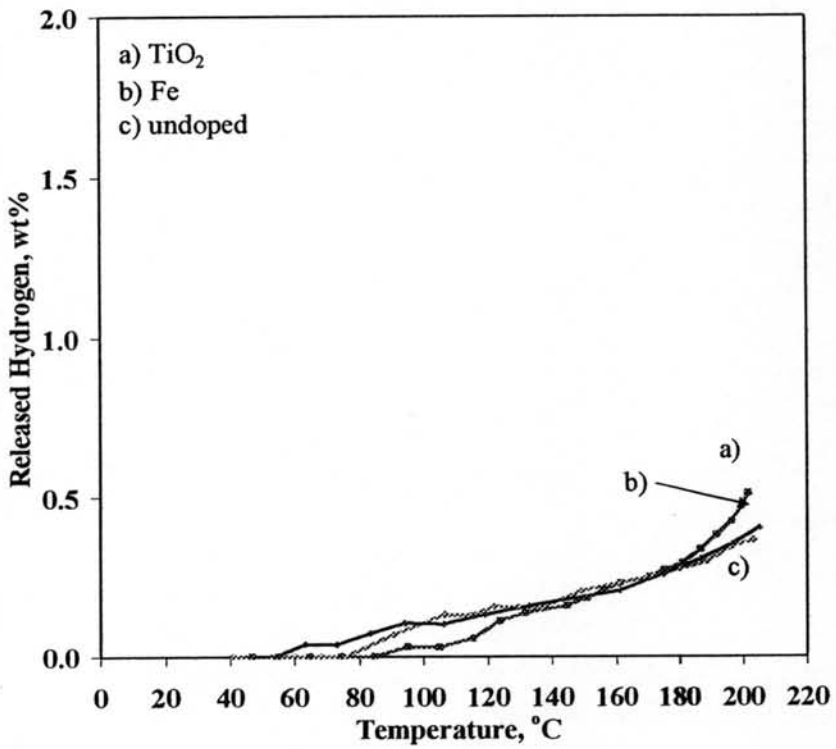

Figure 4.1 Correlation between temperature and hydrogen released during hydrogen desorption from the mixture of $LiNH_2$ and LiH with a 1:1 mol ratio by mortar and pestle for 15 min: a) 1 mol% TiO_2, b) 1 mol% Fe, and c) undoped.

4.1.2 Mixed by Agate Ball Milling

A 1:1 mol ratio of $LiNH_2$ and LiH mixture was added with 1 mol% TiO_2, $ZrCl_4$, Ni, or Fe and mixed by agate ball milling to compare the effect of the catalysts on hydrogen desorption, as shown in Figure 4.2. The results show that the catalysts increase the amount of hydrogen desorption and increase the hydrogen desorption kinetics. The amounts of released hydrogen from the doped samples are significantly higher than the undoped one, which is 0.43 wt%. The samples doped with $ZrCl_4$, Ni and Fe desorb 0.78, 0.76 and 0.68 wt% hydrogen at 200°C, respectively, and give the same rate of hydrogen desorption. However, the sample doped with TiO_2 desorbs 1.5 wt% hydrogen at the same temperature and clearly increases the hydrogen desorption kinetics.

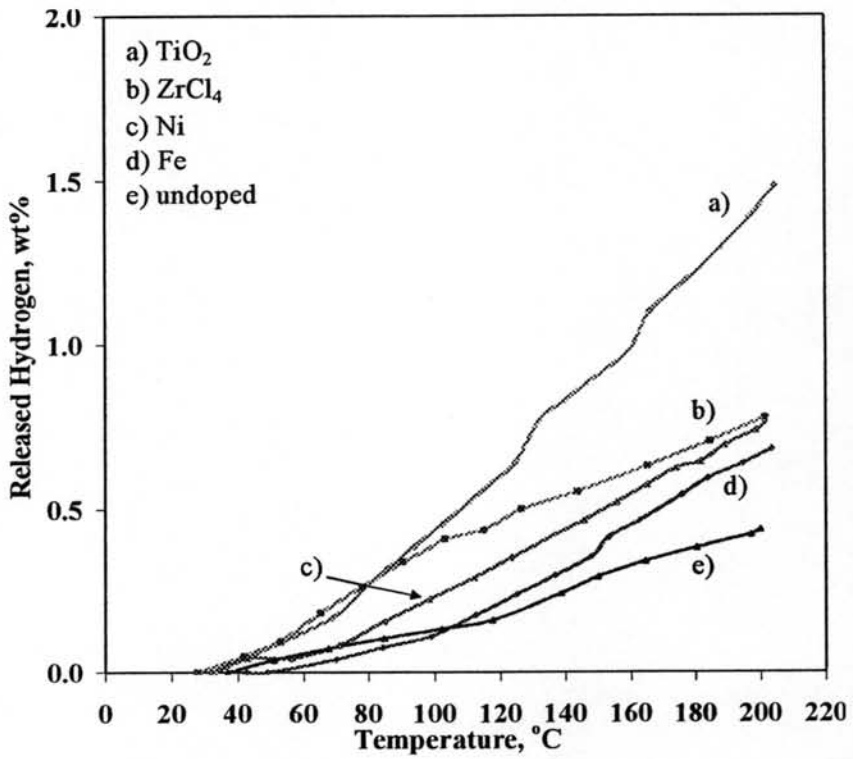

Figure 4.2 Correlation between temperature and hydrogen released during hydrogen desorption from the mixture of $LiNH_2$ and LiH with a 1:1 mol ratio by using agate ball milling for 2 h: a) 1 mol% TiO_2, b) 1 mol% $ZrCl_4$, c) 1 mol% Ni, d) 1 mol% Fe, and e) undoped.

4.2 Effect of Mixing Means on Hydrogen Desorption in Li-N-H Systems

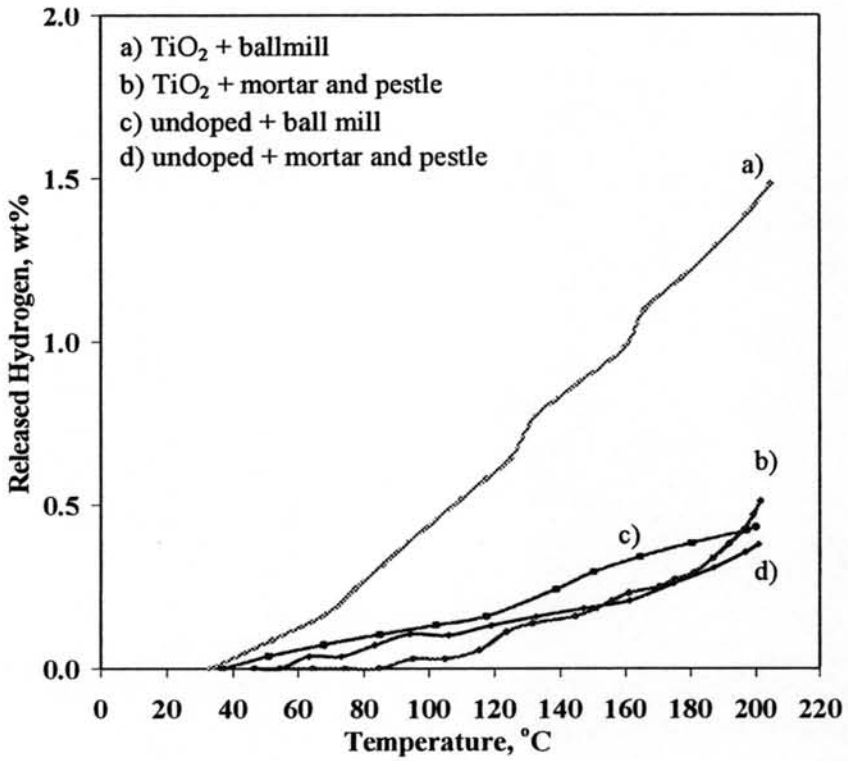

Figure 4.3 Correlation between temperature and hydrogen released during hydrogen desorption from the mixture of $LiNH_2$ and LiH with a 1:1 mol ratio: a) 1 mol% TiO_2 by using agate ball milling for 2 h, b) 1 mol% TiO_2 by using mortar and pestle for 15 min, c) undoped by using agate ball milling for 2 h, and d) undoped by using mortar and pestle for 15 min.

Figure 4.3 shows the temperature program desorption of the mixture of $LiNH_2$ and LiH with a 1:1 mol ratio with different mixing techniques. It was found that the sample doped with 1 mol% TiO_2 (Figure 4.3a) has an outstandingly high amount of released hydrogen, about 1.5 wt% while the amount of released hydrogen of the TiO_2 doping sample mixed by using mortar and pestle (Figure 4.3b) is about 0.5 wt%. In the case of the undoped samples (Figures 4.3c and 4.3d), the samples seem to release hydrogen at the same rate. However, the one mixed by ball milling desorbs hydrogen at a lower temperature because the ball milling can effectively reduce an average particle size and the small particle has a high surface area to release hydrogen. It is clear that not only a catalyst but also a mixing method affect

the hydrogen desorption of the mixture of $LiNH_2$ and LiH. The samples doped with Fe was also studied for its effect but the hydrogen desorption of the samples is not distinguishable by the means of mixing.

After desorption, the samples were re-absorbed under the hydrogen pressure of 500 psi at 180°C for 12 h. It was found that all tested samples are not able to re-absorb hydrogen.

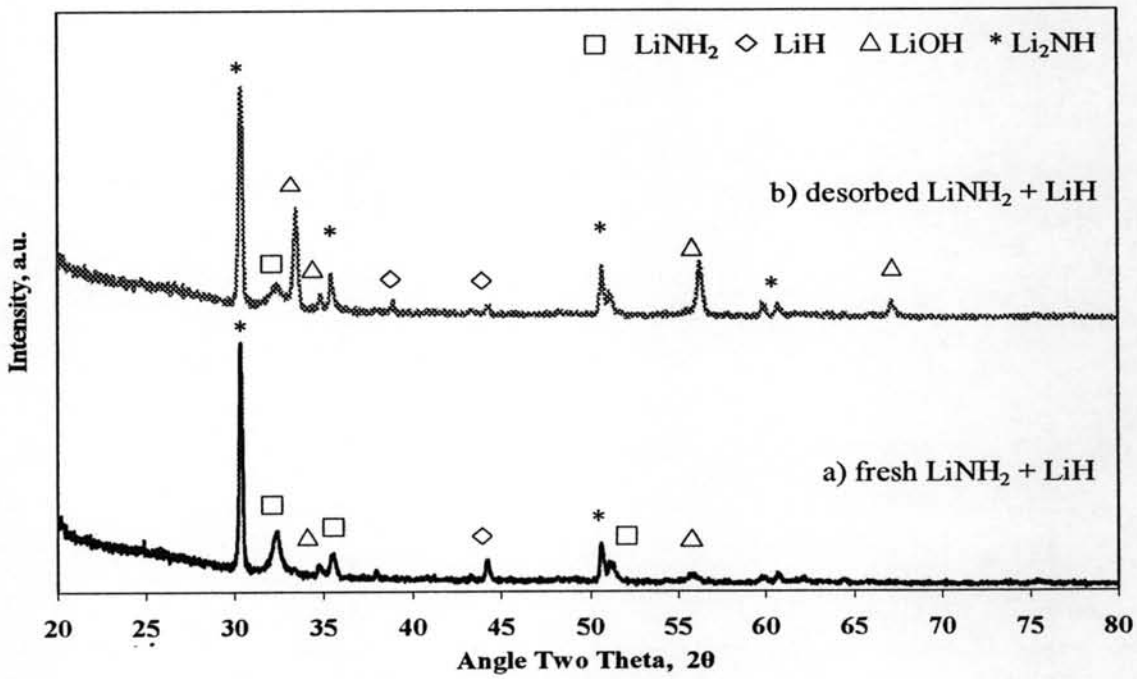

Figure 4.4 XRD patterns of a) fresh $LiNH_2$ and LiH after agate ball milling and b) desorbed $LiNH_2$ and LiH at 200°C.

To find out why the hydrogen desorption of the $LiNH_2$ and LiH mixture is not as high as that reported by Ichikawa *et al.* (2005) (up to 6.5 wt%), characterization by a Rigaku X-ray diffractrometer at room temperature over a range of diffraction angle from 20 – 80 with CuK-alpha radiation (40 kV, 30 mA) is used. Due to the air sensitivity of the samples, before the X-ray diffraction analysis, they were covered with a Kapton tape. Figure 4.4 shows XRD patterns of the mixture of $LiNH_2$ and LiH: a) fresh sample and b) desorbed sample. Results from the XRD patterns supports the results from the temperature program desorption. They show that the main peaks of the fresh sample are Li_2NH, which is a product from the

reaction between $LiNH_2$ and LiH: $LiNH_2 + LiH \leftrightarrow Li_2NH + H_2$ The other peaks with lower intensity indicate LiOH and $LiNH_2$. This implies that the sample has been decomposed before the desorption, possibly during the ball milling. In addition, the sample has many peaks of impurities that would consequently cause the low hydrogen desorption of the $LiNH_2$ and LiH mixture.

To examine the peaks from the XRD pattern of the fresh mixture of $LiNH_2$ and LiH (Figure 4.4a), as-received $LiNH_2$, fresh $LiNH_2$ after agate ball milling, and as-received LiH were characterized by XRD. Figure 4.5 shows XRD patterns of the undoped $LiNH_2$ sample: a) as-received sample; b) milled sample. The XRD patterns show that the main peaks of fresh $LiNH_2$ after ball milling (Figure 4.5b) are Li_2NH and intensity of $LiNH_2$ decreases compared with the as-received one (Figure 4.5a). This substantiates that $LiNH_2$ is decomposed to Li_2NH during the milling.

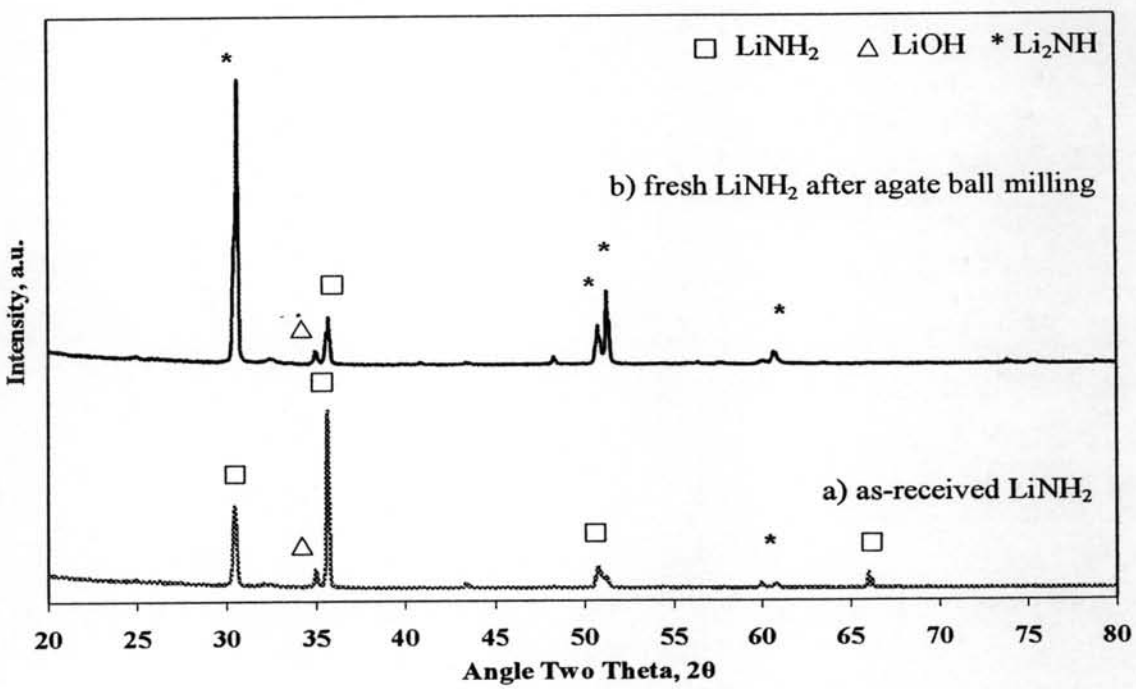

Figure 4.5 XRD patterns of a) as-received $LiNH_2$ and b) fresh $LiNH_2$ after agate ball milling for 2 h.

The XRD pattern of as-received LiH in Figure 4.6 shows very high intensity of LiOH, which occurs by reacting with air or moisture. LiH in this system is not pure enough for further study of the $LiNH_2$ and LiH reaction.

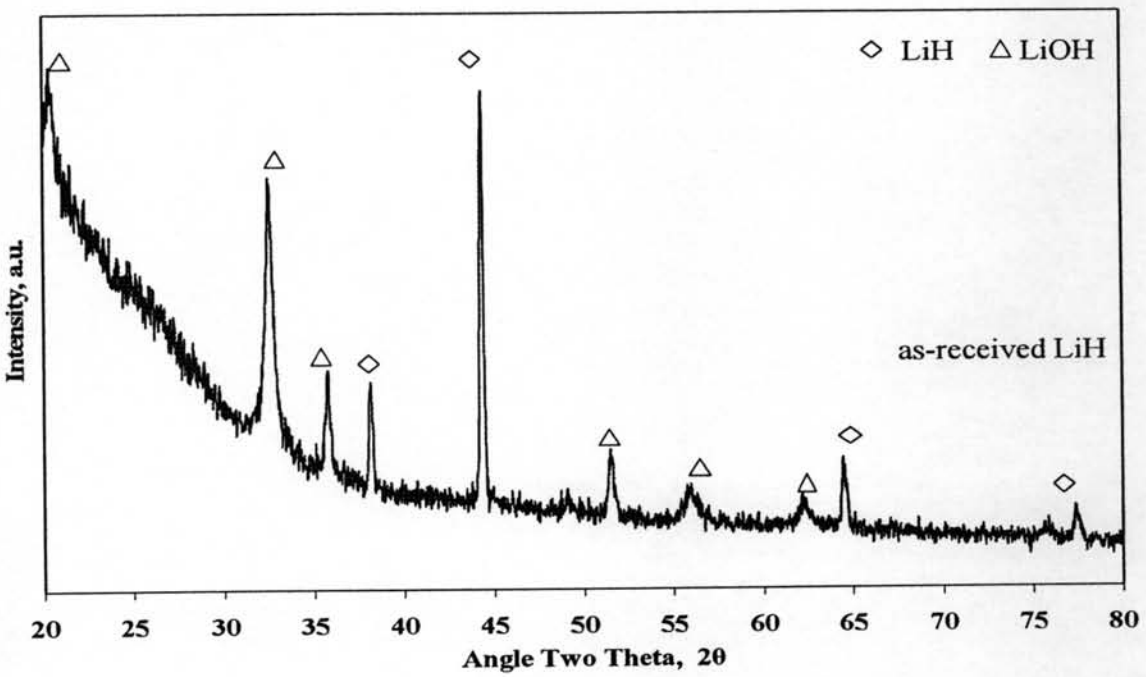

Figure 4.6 XRD patterns of as-received LiH.

4.3 Effect of $LiAlH_4$ on Hydrogen Desorption in $LiNH_2$

XRD patterns of the undoped $LiAlH_4$ sample at different conditions: a) as-received, b) fresh sample after milling, and c) desorbed sample at 200°C, are illustrated in Figure 4.7. After the milling, intensity of $LiAlH_4$ decreases and some peaks of $LiAlH_4$ disappear. Progressive hydrogen desorption at 200°C shows complete desorption of the hydride to LiH and Al. Furthermore, the increase in the intensity and narrow peak of aluminum and LiH show the formation of their crystallites. LiH in higher intensity can also be seen. Because of the decomposition of $LiAlH_4$ to LiH, $LiAlH_4$ was used as a source of LiH to react with $LiNH_2$.

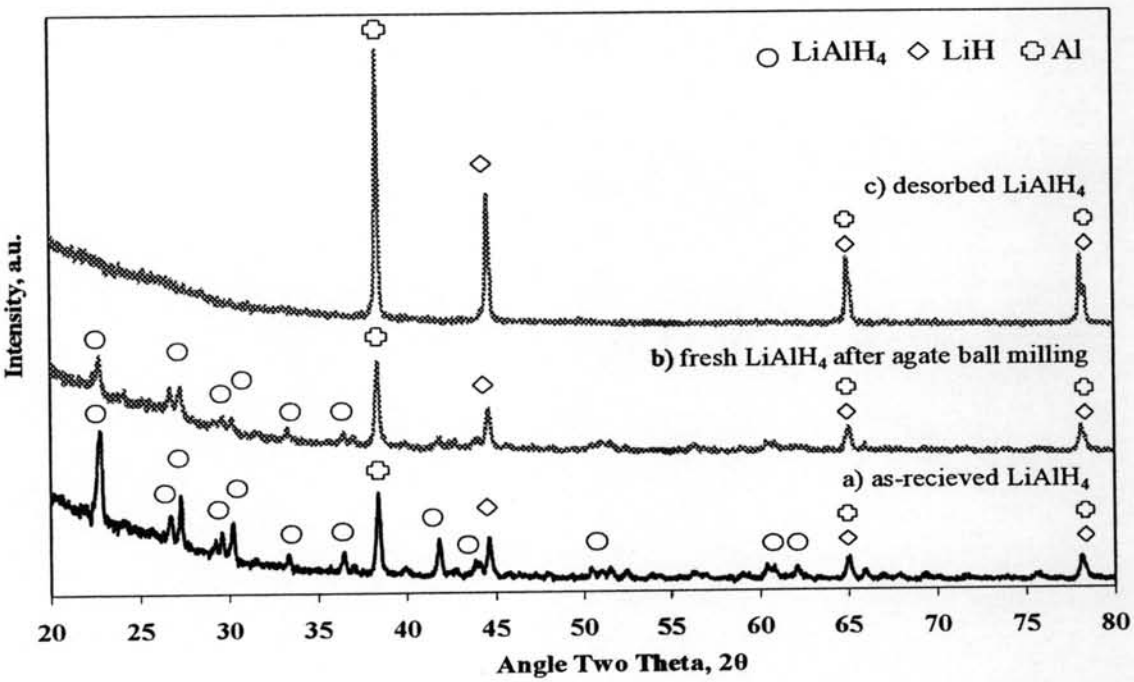

Figure 4.7 XRD patterns of a) as-received $LiAlH_4$, b) fresh $LiAlH_4$ after milling, and c) desorbed $LiAlH_4$ at 200°C.

Figure 4.8 shows the hydrogen desorption of 1:1, 1:3, and 1:5 mol ratios of $LiNH_2$ and $LiAlH_4$ compared with pure $LiAlH_4$ and pure $LiNH_2$. The result shows that pure $LiAlH_4$ gives the highest hydrogen evolution rate when temperature reaches about 120°C and releases about 9.3 wt% hydrogen at 200°C followed by the 1:5 mol ratio sample, 5.0 wt%. The amounts of hydrogen desorption of samples with 1:3 and 1:1 mol ratios are almost the same, about 2.5 wt%. With the increase in the $LiAlH_4$ loading, the hydrogen desorption behavior is similar to that of pure $LiAlH_4$. However, the amount of hydrogen desorption of the 1:5 mol ratio is less than that of pure $LiAlH_4$. In this case, the explanation is that $LiNH_2$ in the mixture may somehow affect the decomposition of $LiAlH_4$ during the milling. The XRD patterns in Figures 4.7b and 4.9a confirm that the fresh 1:5 mol ratio sample (Figure 4.9a) has lower peaks of $LiAlH_4$ than those of pure $LiAlH_4$ (Figure 4.7b) meaning that $LiNH_2$ in the 1:5 mol ratio sample has an effect on the decomposition of $LiAlH_4$. Comparison among the decomposition slopes, the three mixtures of $LiNH_2$ and $LiAlH_4$ with pure $LiNH_2$, shows that the formers are not as steep as the latter. A possible reason may be, during the decomposition of $LiNH_2$ to NH_3, NH_3 is consumed by the reaction

with LiH from $LiAlH_4$ resulting in a lower total pressure. In the case of the 1:5 mol ratio sample, its slope at low temperatures is still lower than that of pure $LiNH_2$. However, as the temperature is high enough, excess LiH is formed from the decomposition of $LiAlH_4$ resulting in the higher reaction rate between LiH and NH_3. And because of that, its slope is not as high as that of $LiAlH_4$ decomposition.

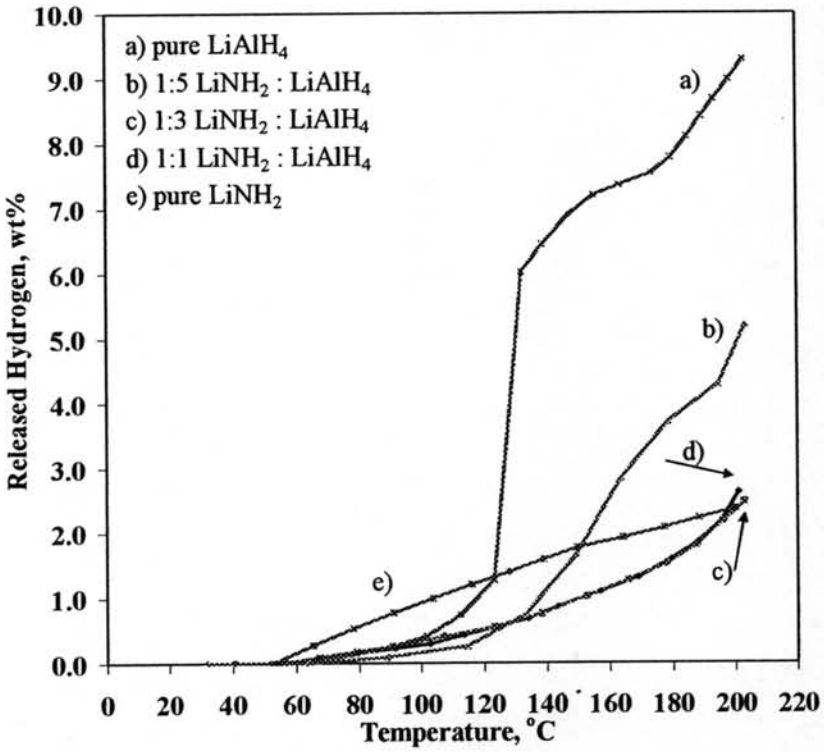

Figure 4.8 Temperature program desorption from room temperature to 200°C with the heating rate of 2°C min^{-1} by using agate ball milling for 1 h: a) pure $LiAlH_4$ b) 1:5 mol ratio of $LiNH_2$ and $LiAlH_4$ c) 1:3 mol ratio of $LiNH_2$ and $LiAlH_4$ d) 1:1 mol ratio of $LiNH_2$ and $LiAlH_4$, and e) pure $LiNH_2$.

XRD patterns of fresh and desorbed 1:5 mol ratio of $LiNH_2$ and $LiAlH_4$ in Figure 4.9 show that the fresh sample (Figure 4.9a) still has some peaks of $LiAlH_4$ to decompose to LiH and then reacts with $LiNH_2$. However, based on the results, it is not possible to specify whether hydrogen is from the composition of $LiAlH_4$ or reaction of the $LiNH_2$ and LiH, or both. XRD patterns of fresh and desorbed samples with 1:1 and 1:3 mol ratios of $LiNH_2$ and $LiAlH_4$ are the same.

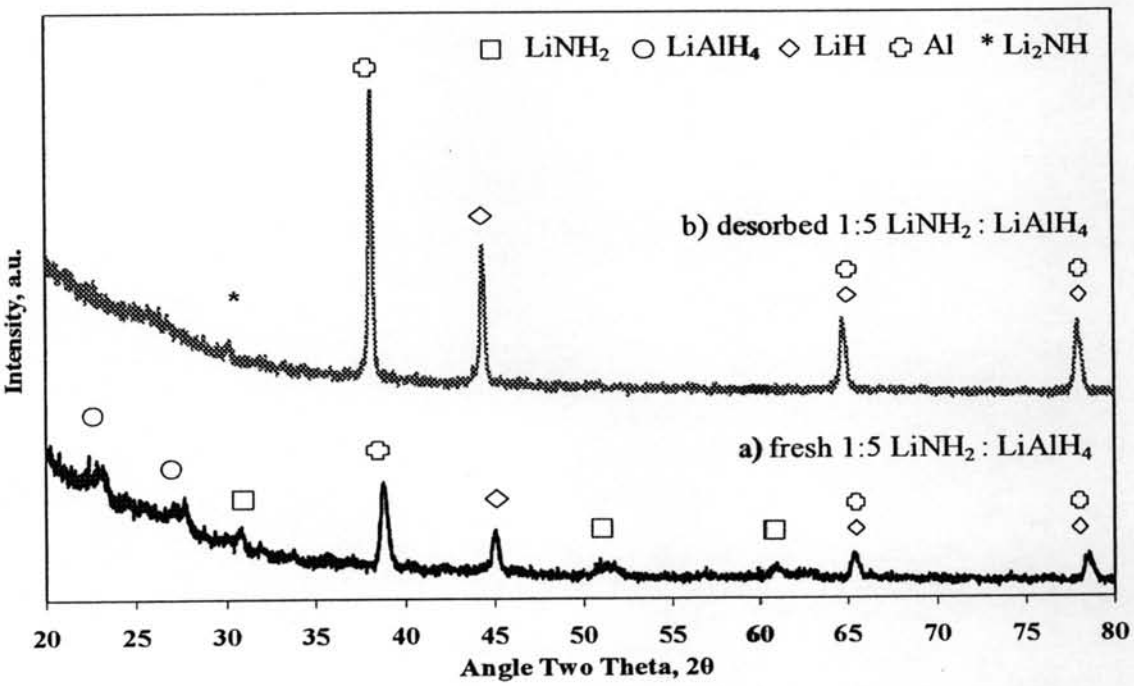

Figure 4.9 XRD patterns of a 1:5 mol ratio of $LiNH_2$ and $LiAlH_4$: a) fresh after ball milling and b) desorbed at 200°C.

4.4 Effect of Catalysts on Hydrogen Desorption in Li-Al-N-H Systems

4.4.1 Effect of Catalysts

To study the effect of catalyst types on hydrogen desorption from the mixture of $LiNH_2$ and $LiAlH_4$, $ZrCl_4$ and TiO_2 were used. Zidan *et al.* (1999) reported that Zr and Ti affected the hydrogenation/dehydrogenation of $NaAlH_4$ so some physical properties and mechanisms of Zr and Ti may affect $LiAlH_4$. Figure 4.10 shows the hydrogen desorption of the 1:5 mol ratio of $LiNH_2$ and $LiAlH_4$ doped with 4 mol% $ZrCl_4$ or TiO_2 compared with the undoped one mixed with agate ball milling. The figure clearly confirms that the catalysts enhance the kinetics of the hydrogen desorption. The $ZrCl_4$ doped sample (Figure 4.10a) shows a higher amount of hydrogen desorbed, 8.0 wt% at 200°C, than the sample doped with TiO_2 (Figure 4.10c) and the undoped one (Figure 4.10b), both around 5.0 wt%. The addition of $ZrCl_4$ increases the amount of hydrogen desorption and desorption kinetics while TiO_2 only increases the desorption kinetics.

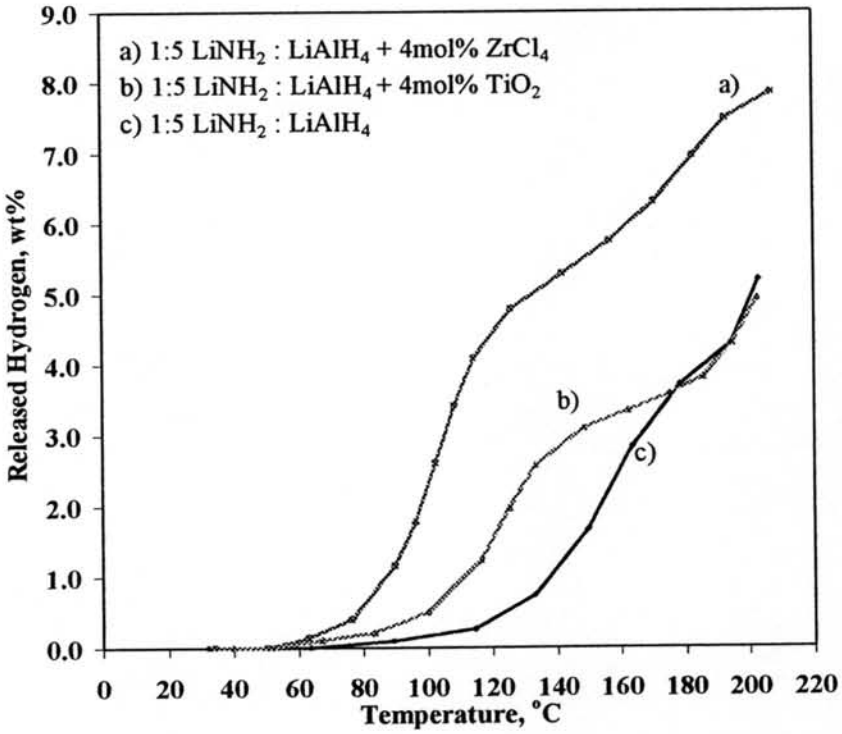

Figure 4.10 Temperature program desorption of a 1:5 mol ratio of $LiNH_2$ and $LiAlH_4$ mixed by using agate ball milling for 1 h: a) doped with 4 mol% $ZrCl_4$, b) doped with 4 mol% TiO_2, and c) undoped.

XRD results of 1:5 $LiNH_2$:$LiAlH_4$ doped with 4 mol% TiO_2 or 4 mol% $ZrCl_4$ after hydrogen desorption are shown in Figures 4.11 and 4.12, respectively. Comparison of the XRD patterns of the undoped sample (Figure 4.9) and the one doped with TiO_2 or $ZrCl_4$ shows that only the sample doped with $ZrCl_4$ resulted in the presence of LiCl after the milling. This may be due to the reaction of LiH with $ZrCl_4$ when the amount of $ZrCl_4$ is high enough, 4 mol% for this case, to form LiCl. After complete desorption, the XRD results show the increase in the formation of LiH and Al for all samples (Figures 4.9b, 4.11b, and 4.12b). Lastly, we do not observe any peaks of the transition metal compound (Zr and Ti) in the samples after the hydrogen desorption/absorption by the X-ray diffraction technique.

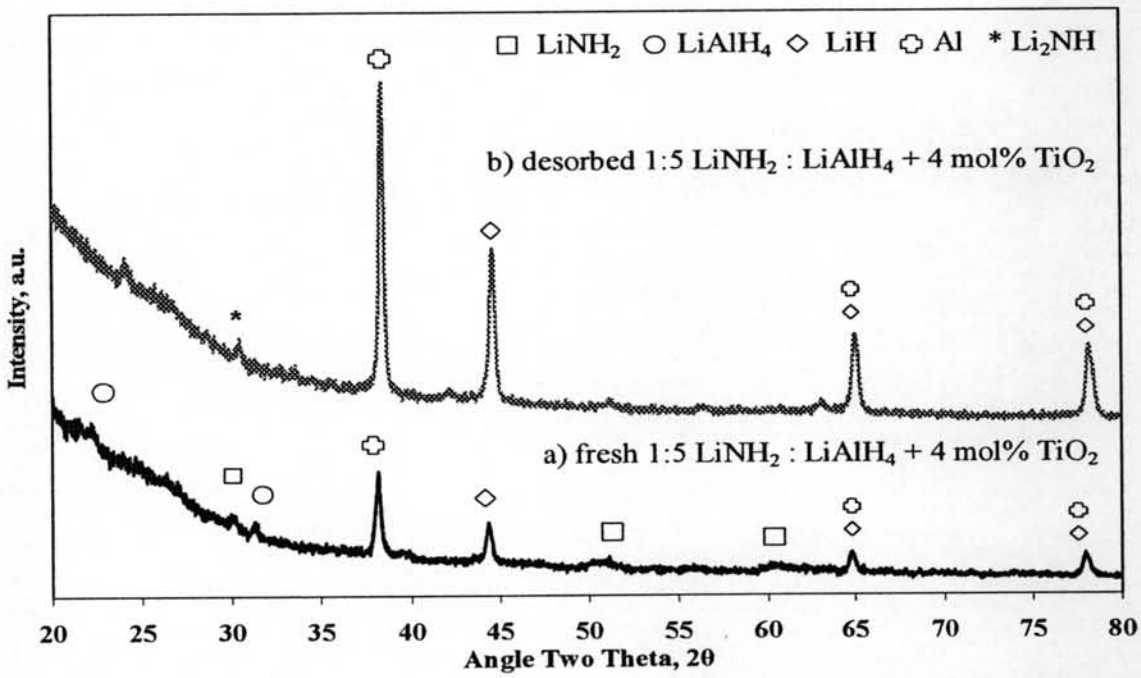

Figure 4.11 XRD patterns of 4 mol% TiO_2-1:5 mol ratio of $LiNH_2$ and $LiAlH_4$: a) fresh after ball milling and b) desorbed at 200°C.

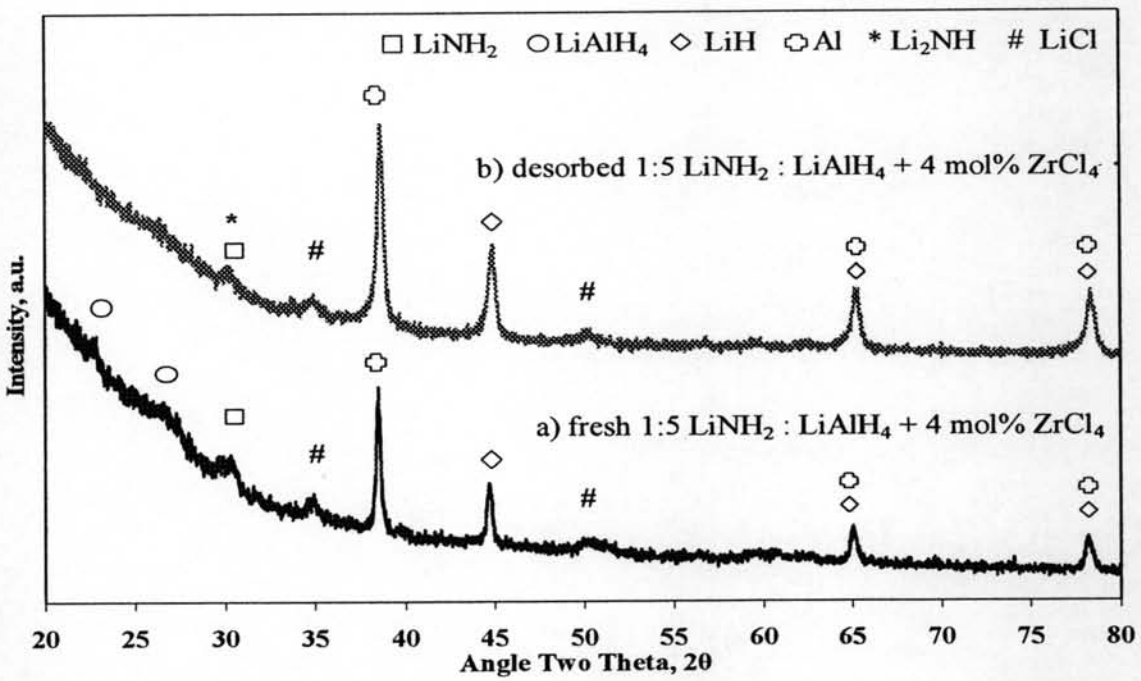

Figure 4.12 XRD patterns of 4 mol% $ZrCl_4$-1:5 mol ratio of $LiNH_2$ and $LiAlH_4$: a) fresh after ball milling, b) desorbed at 200°C, and c) absorbed at 180°C.

4.4.2 Effect of $ZrCl_4$ Loading

Amounts of $ZrCl_4$ doped on the 1:5 mol ratio of $LiNH_2$ and $LiAlH_4$ are at 1 and 4 mol%. Its dehydrogenation from room temperature to 200°C with the heating rate of 2°C min^{-1} is shown in Figure 4.13. From the figure, only a small amount of $ZrCl_4$ can enhance the desorption kinetics. The higher amount of $ZrCl_4$ loading increases the desorption kinetics and hydrogen capacity. However, although the desorption temperature of the samples with the two loading are relatively the same, they are lower than that of the undoped sample. At the 4 mol% $ZrCl_4$ loading, the hydride starts to decompose at 55°C and releases 8.0 wt% hydrogen at 200°C.

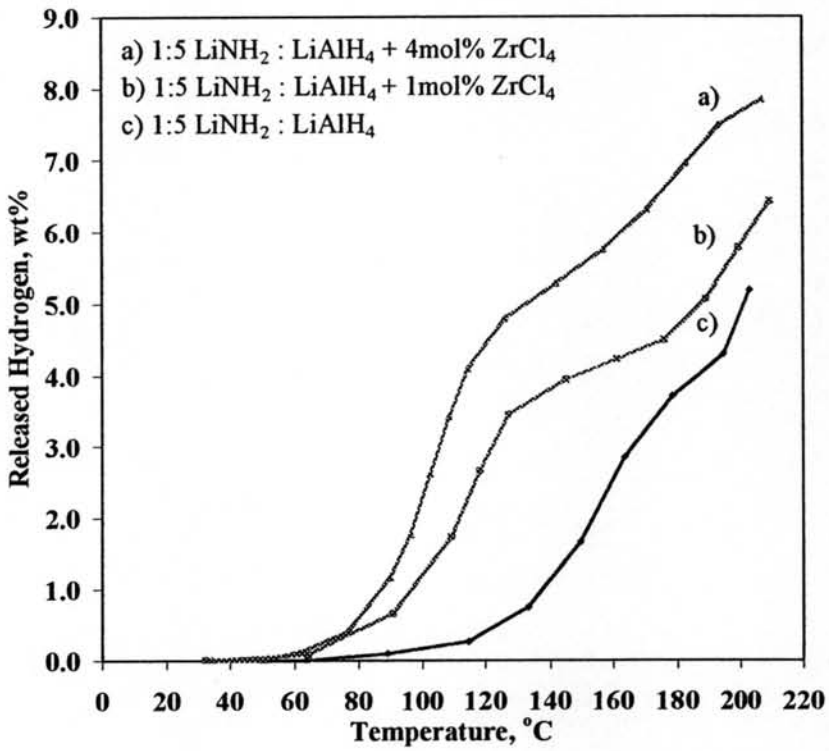

Figure 4.13 Temperature program desorption of a 1:5 mol ratio of $LiNH_2$ and $LiAlH_4$ mixed by using agate ball milling for 1 h: a) doped with 4 mol% $ZrCl_4$, b) doped with 1 mol% $ZrCl_4$, and c) undoped.

4.4.3 Reversibility of Li-Al-N-H Systems

To study the reversibility and stability of hydrogen desorption/absorption of the mixture of $LiAlH_4$ and $LiNH_2$, a sample is dehydrogenated from room temperature to 200°C with the heating rate of 2°C min^{-1}. The first dehydrogenation of 1:1 $LiNH_2$ and $LiAlH_4$ releases about 2.6 wt% hydrogen. After the first desorption, the sample was reabsorbed under 1,500 psi of hydrogen pressure at 180°C for 12 h. The amount of released hydrogen drops to 0.4 wt% for the subsequent desorptions, as shown in Figures 4.14. We observed that the decomposition temperature has been shifted from 50°C to 70°C after the first cycle. For other experiments of $LiNH_2$ and $LiAlH_4$ mixtures such as the 1:1 mol ratio doped with 1 mol% $ZrCl_4$, or 1:3, or 1:5 undoped or doped with 1 and 4 mol% $ZrCl_4$, only 0.15 – 0.4 wt% can be reabsorbed.

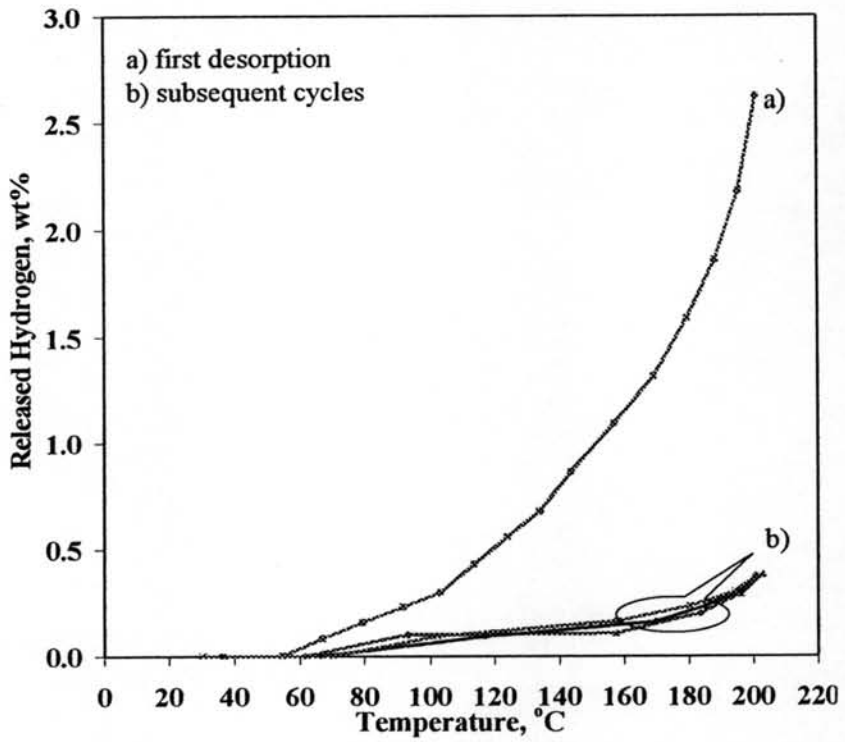

Figure 4.14 Temperature program desorption from the mixture of $LiNH_2$ and $LiAlH_4$ with a 1:1 mol ratio by using agate ball milling for 1 h: a) first cycle and b) subsequent cycles.

The total reversibility of the desorbed samples could not be achieved to their original states. The assumption for the reversibility of the Li-Al-N-H system is from the reaction between $LiNH_2$ and LiH but after absorption (Figure 4.15c), the $LiNH_2$ disappears and only Al and LiH are present. XRD patterns of other studied samples with different $LiNH_2$ to $LiAlH_4$ ratios and different catalysts are more or less the same.

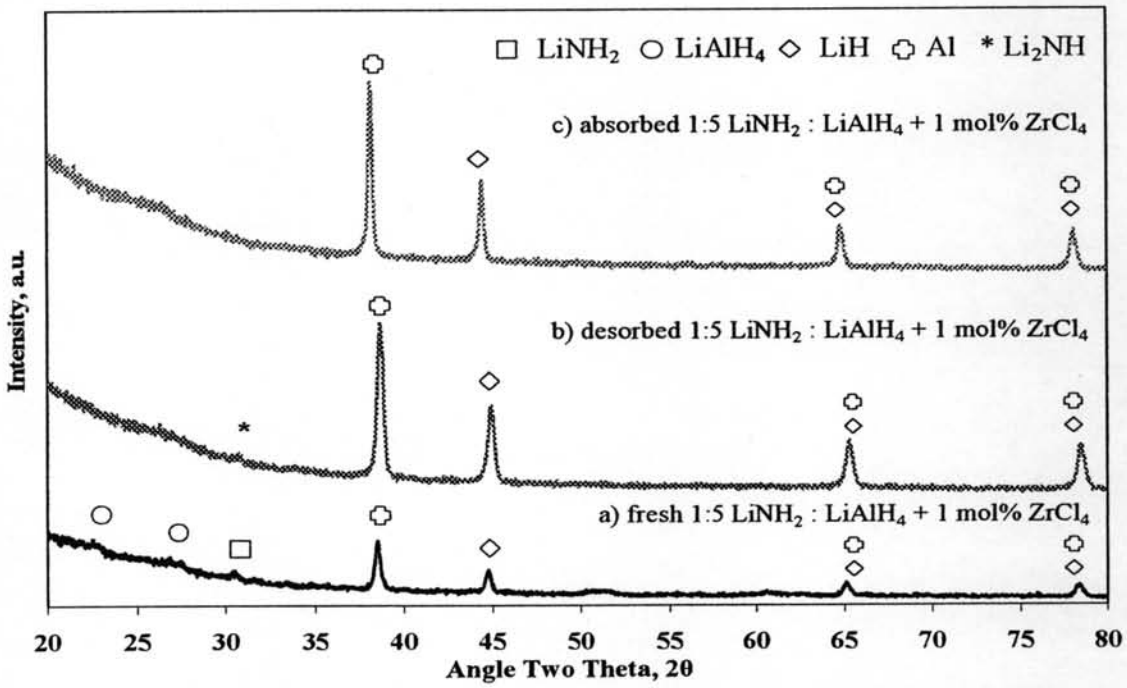

Figure 4.15 XRD patterns of 1 mol% $ZrCl_4$-1:5 mol ratio of $LiNH_2$ and $LiAlH_4$: a) fresh after ball milling, b) desorbed at 200°C, and c) absorbed at 180°C.

4.4.4 Effect of Sample Loading Methods

As NH_3 for the decomposition of $LiNH_2$ is expected to react with LiH from $LiAlH_4$, different sample loading methods were studied. The method is similar to Ichikawa *et al.* (2004). Here, three configurations were used. Configuration A is to place $LiAlH_4$ milled with 4 mol% $ZrCl_4$ on top of $LiNH_2$ milled with 4 mol% $ZrCl_4$ with a 1:5 mol ratio of $LiNH_2$ to $LiAlH_4$. Configuration B is to place $LiAlH_4$ milled with 4 mol% $ZrCl_4$ on top of $LiNH_2$ with a 1:5 mol ratio of $LiNH_2$ to $LiAlH_4$. In configuration C, 1:5 $LiNH_2$:$LiAlH_4$ doped with 4 mol% $ZrCl_4$ is used without the separation of each hydride. Figure 4.16 shows the configurations of a 1:5 mol ratio of

$LiNH_2$ and $LiAlH_4$. We can see that the first two configurations are based on the postulation that NH_3 from $LiNH_2$ passes through the bed of $LiAlH_4$ and react with LiH to form H_2 while the last configuration is to mix these constituents homogeneously.

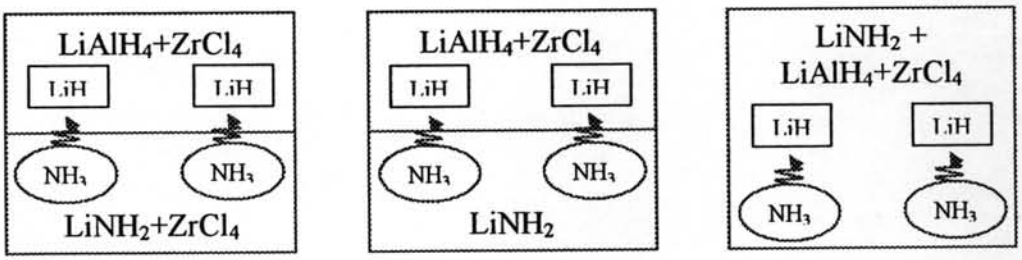

Figure 4.16 Packing configuration of $LiNH_2$ and $LiAlH_4$ mixtures: a) two-layered sample both of which doped with 4 mol% $ZrCl_4$, b) two-layered sample and only $LiAlH_4$ doped with 4 mol% $ZrCl_4$, and c) both hydrides mixed with 4 mol% $ZrCl_4$.

Figure 4.17 shows the temperature program desorption between different sample loading methods. For the configurations A and B, it should be noted that the shape of the hydrogen emission curve in Figure 4.17a is quite similar to that of Figure 4.17b. In addition, the amounts of released hydrogen are not significantly different. For the $LiNH_2$ phase, the doping of $ZrCl_4$ barely changes the hydrogen desorption behavior. In other words, $ZrCl_4$ does not have any influence on the hydrogen desorption or desorption kinetics on $LiNH_2$. By comparing the results of the two-layered samples (Figures 4.17a and 4.17b) and one-layered one (Figure 4.17c), it indicates that the contact time is one important parameter to improve the hydrogen desorption. NH_3 from $LiNH_2$ should have long enough resident time to react with LiH from $LiAlH_4$. In the case of $LiNH_2$ mixed together with $LiAlH_4$ (Figure 4.17c), $LiNH_2$ in the mixture has an effect on the decomposition of $LiAlH_4$ during the milling, as explained in Figure 4.8, Ichikawa *et al.* (2004b) concluded that LiH plays a role for the decomposition of $LiNH_2$ from the study between $LiNH_2$ and LiH compared with two-layer undoped $LiNH_2$ and LiH.

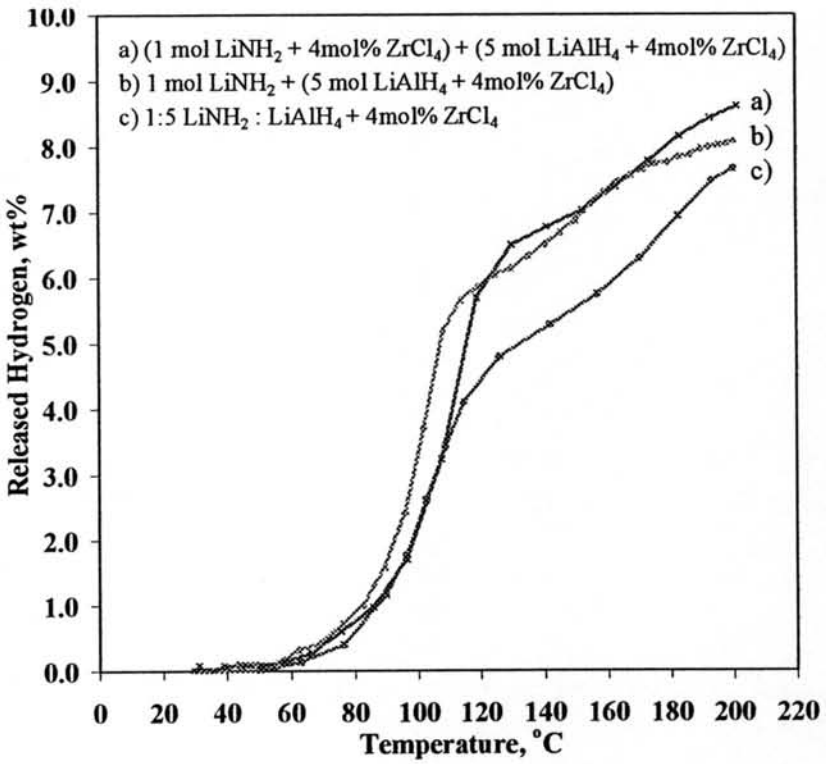

Figure 4.17 Correlation between temperature and hydrogen capacity, during hydrogen desorption on a 1:5 mol ratio of $LiNH_2$ and $LiAlH_4$: a) two-layered sample each of which doped with 4 mol% $ZrCl_4$, b) two-layered sample only $LiAlH_4$ doped with 4 mol% $ZrCl_4$, and c) one-layered sample doped with 4 mol% $ZrCl_4$.

Effects of different catalysts on the two-layered 1:1 $LiNH_2$ and $LiAlH_4$ doped with 4 mol% VCl_3 are shown in Figure 4.18a, and the two-layered doped with 4 mol% $ZrCl_4$ (Figure 4.18b) shows higher amounts of hydrogen desorption and reaction rates than those of the one-layered (Figure 4.18c). It is not only caused by the effect of the transition metals but also caused by the packing configuration. VCl_3 seems to be the most effective additive to increase the hydrogen desorption and the desorption kinetics.

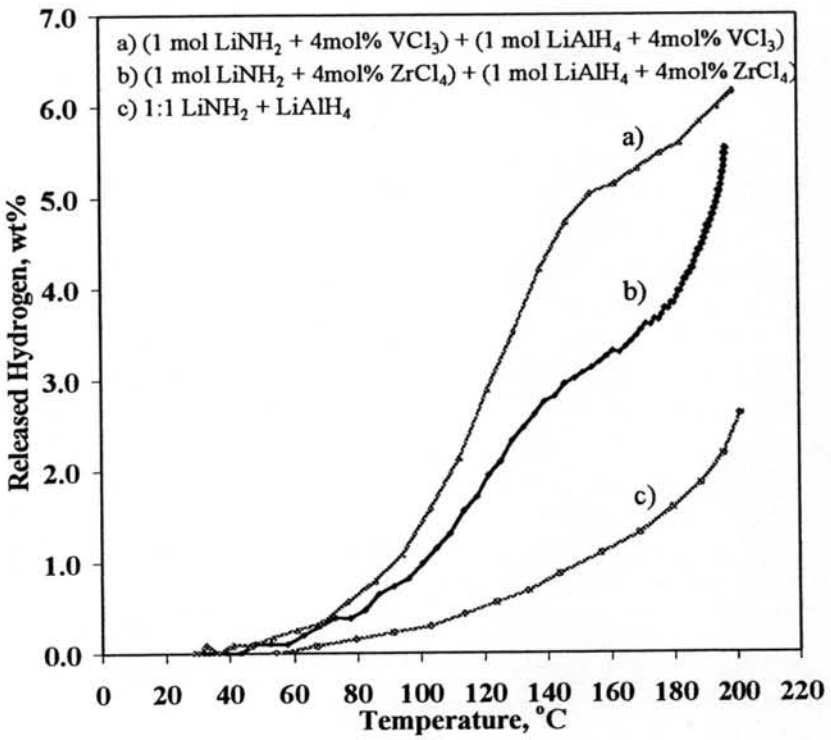

Figure 4.18 Correlation between temperature and hydrogen capacity, during hydrogen desorption on a 1:1 mol ratio of $LiNH_2$ and $liAlH_4$: a) two-layered sample which are doped with 4 mol% VCl_3, b) two-layered sample which are doped with 4 mol% $ZrCl_4$, and c) undoped.

XRD patterns of each layer, $LiNH_2$ doped with 4 mol% VCl_3 and $LiAlH_4$ doped with 4 mol% VCl_3, are shown in Figures 4.19 and 4.20, respectively. The samples of these figures are doped with 4 mol% of chloride forms, like Figure 4.12, then LiCl are observed and any peaks of the transition metal compounds, V or Zr, in the samples are not seen. The XRD patterns explain the results from Figure 4.17 that the transition metals have an effect on the hydrogen desorption. While the XRD patterns of the hydrogen absorption of all samples are not different as shown in Figures 4.15, hydrogen can be desorbed in the subsequent cycle in the range of 0.15 to 0.4 wt%.

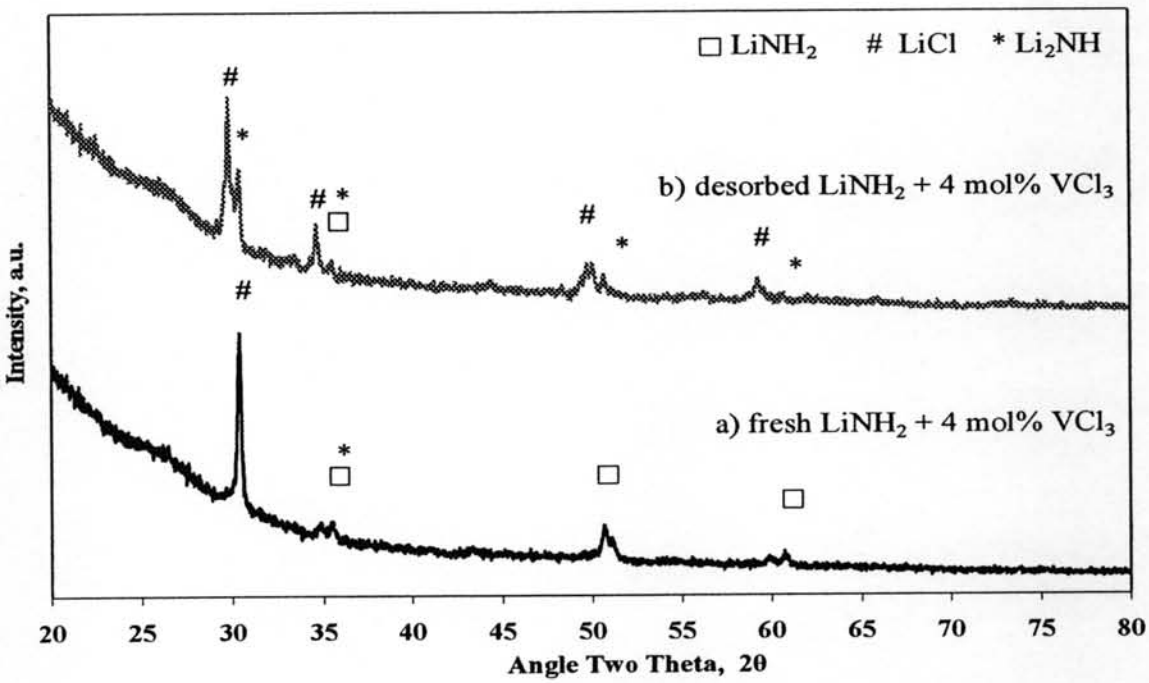

Figure 4.19 XRD patterns of 4 mol% $ZrCl_4$-$LiNH_2$: a) fresh after ball milling and b) desorbed at 200°C.

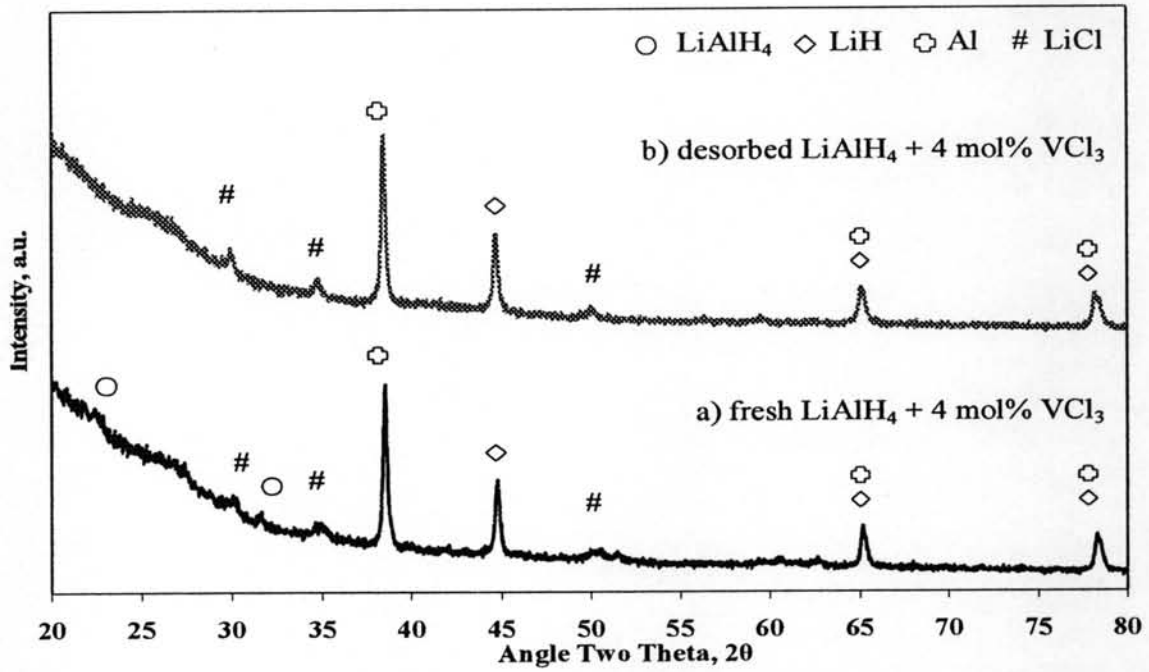

Figure 4.20 XRD patterns of 4 mol% $ZrCl_4$-$LiAlH_4$: a) fresh after ball milling and b) desorbed at 200°C.

4.5 TPD and MS of $LiNH_2$ and $LiNH_2/LiAlH_4$

4.5.1 Effect of Catalyst on $LiNH_2$

Figures 4.21 shows the TPD-MS patterns of $LiNH_2$ milled with and without 4 mol% $ZrCl_4$ for 1 h. The undoped sample desorbs ammonia (m/z = 17) between 250 - 700°C with a significant peak at 500°C. For $LiNH_2$ doped with 4 mol% $ZrCl_4$, ammonia desorbs in the temperature range of 150 – 650°C and the intensity of ammonia is much lower than that of the undoped sample.

Figure 4.22 shows the hydrogen desorption from $LiNH_2$ milled with and without 4 mol% $ZrCl_4$. The undoped sample desorbs hydrogen (m/z = 2) between 450 – 650°C while the sample doped with 4 mol% $ZrCl_4$ desorbs hydrogen between 350 – 650 °C and the relative intensity is higher than that of the undoped sample.

Results from both figures show that the catalyst decreases the temperatures of the ammonia emission while it does not significantly affect on the temperature of the hydrogen emission. The catalyst does not only decrease the ammonia emission, it also increases the hydrogen desorption from $LiNH_2$.

4.5.2 Effect of $LiAlH_4$ Loading

Comparison of the TPD-MS between the ball milled $LiNH_2$ and a 1:1 mol ratio of $LiNH_2$ and $LiAlH_4$ (Figure 4.23) shows that the 1:1 mol ratio sample decomposes at significantly lower temperatures than the ball milled $LiNH_2$. The mixture starts to desorb ammonia at 100 °C and completes the desorption around 550°C. This may be due to LiH from $LiAlH_4$ accelerates the decomposition of $LiNH_2$. This result is consistent with that of Ichkawa *et al.* (2004b).

Decomposition of 1:1 and 1:5 mol ratios of $LiNH_2$ and $LiAlH_4$ is shown in Figures 4.24 to 4.26. Figure 4.24 shows that the 1:5 mol ratio sample desorbs ammonia in the temperature range of 100 – 550°C with high ammonia intensity at 200, 300 and 550°C while the 1:1 mol ratio one desorbs ammonia with much less intensity.

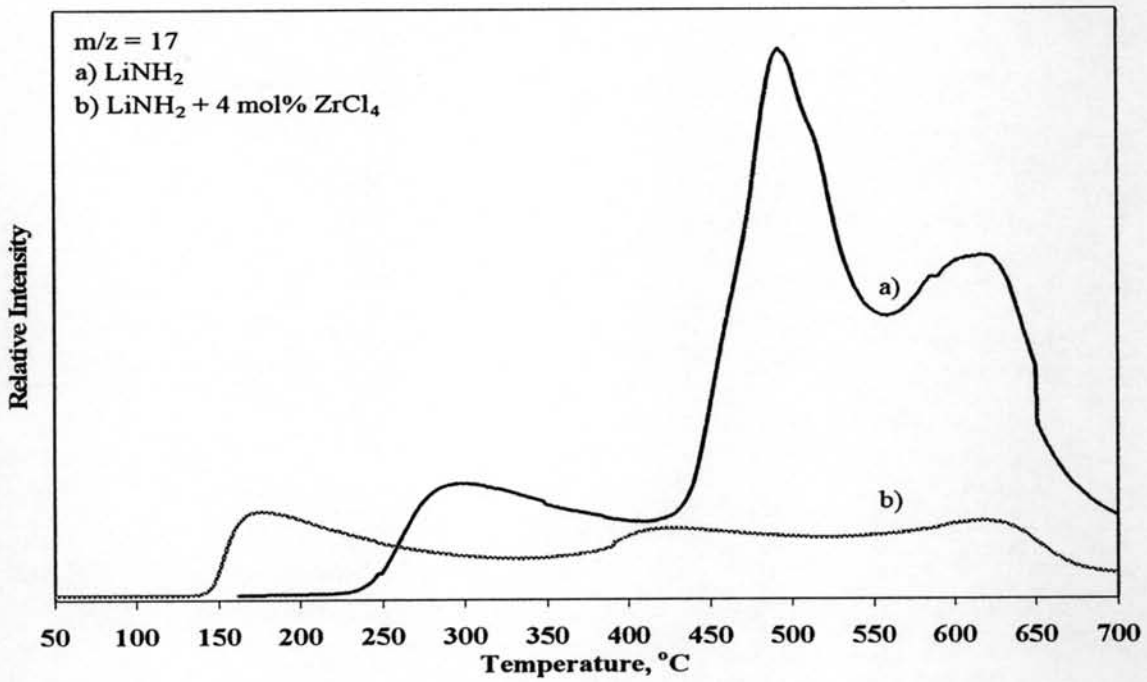

Figure 4.21 TPD-MS patterns of ammonia (m/z = 17) from $LiNH_2$: a) undoped and b) doped with 4 mol% $ZrCl_4$.

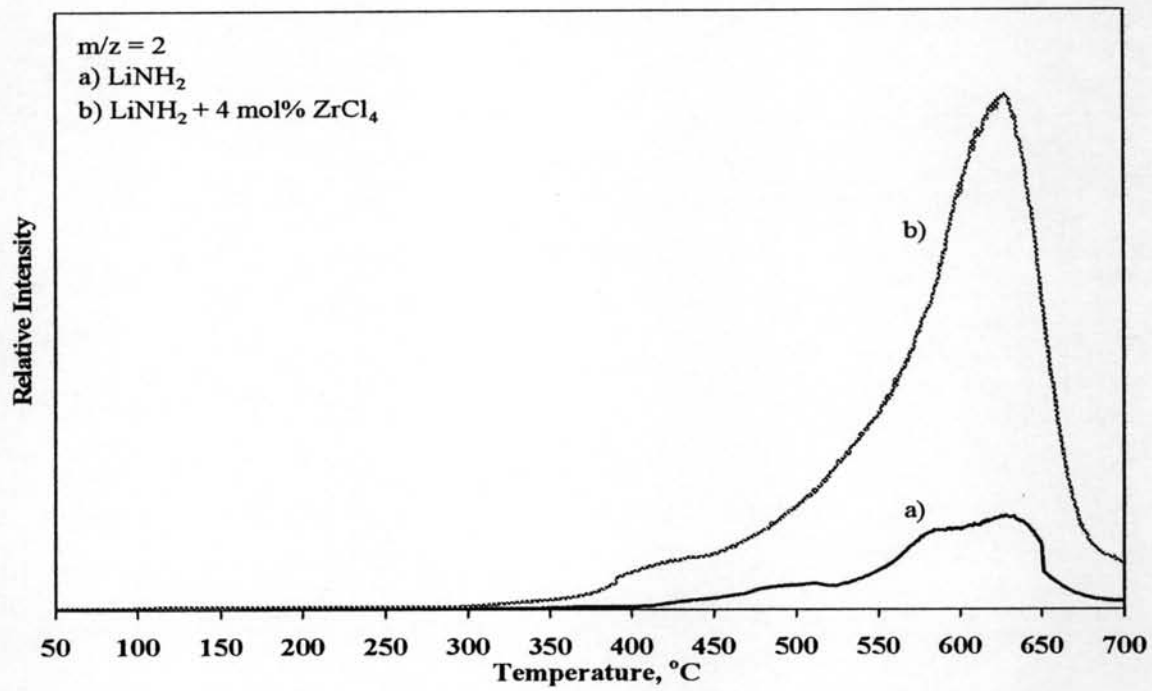

Figure 4.22 TPD-MS patterns of hydrogen (m/z = 2) from $LiNH_2$: a) undoped and b) doped with 4 mol% $ZrCl_4$.

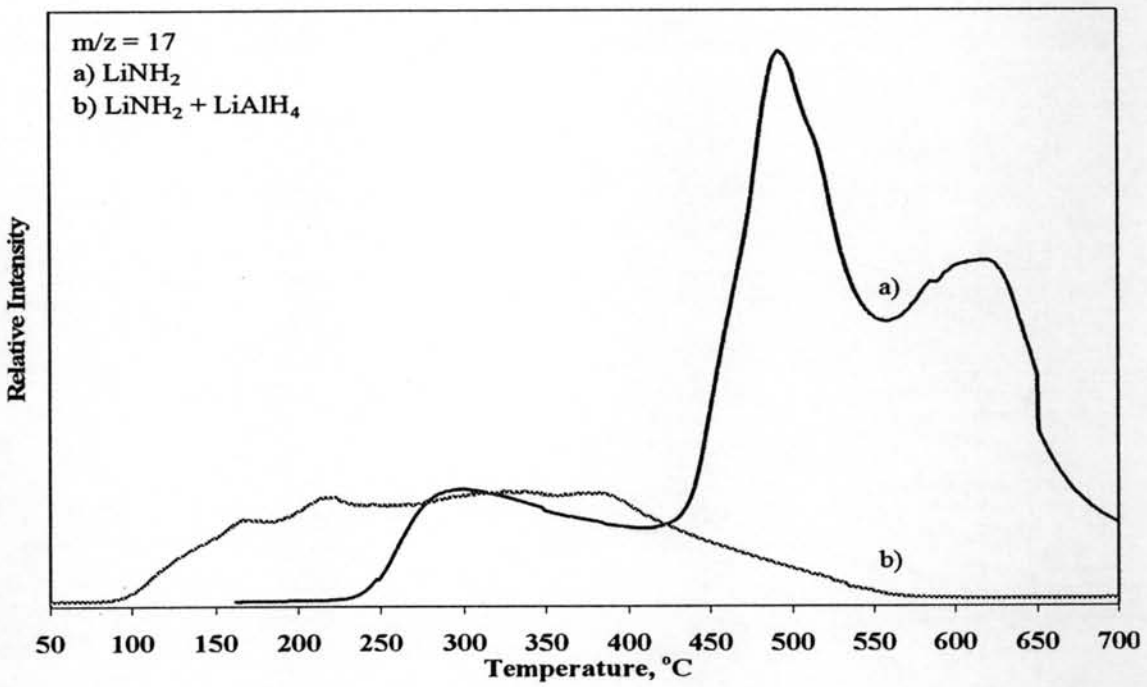

Figure 4.23 TPD-MS patterns of ammonia (m/z = 17) from: a) pure $LiNH_2$ and b) 1:1 mol ratio of $LiNH_2$ and $LiAlH_4$.

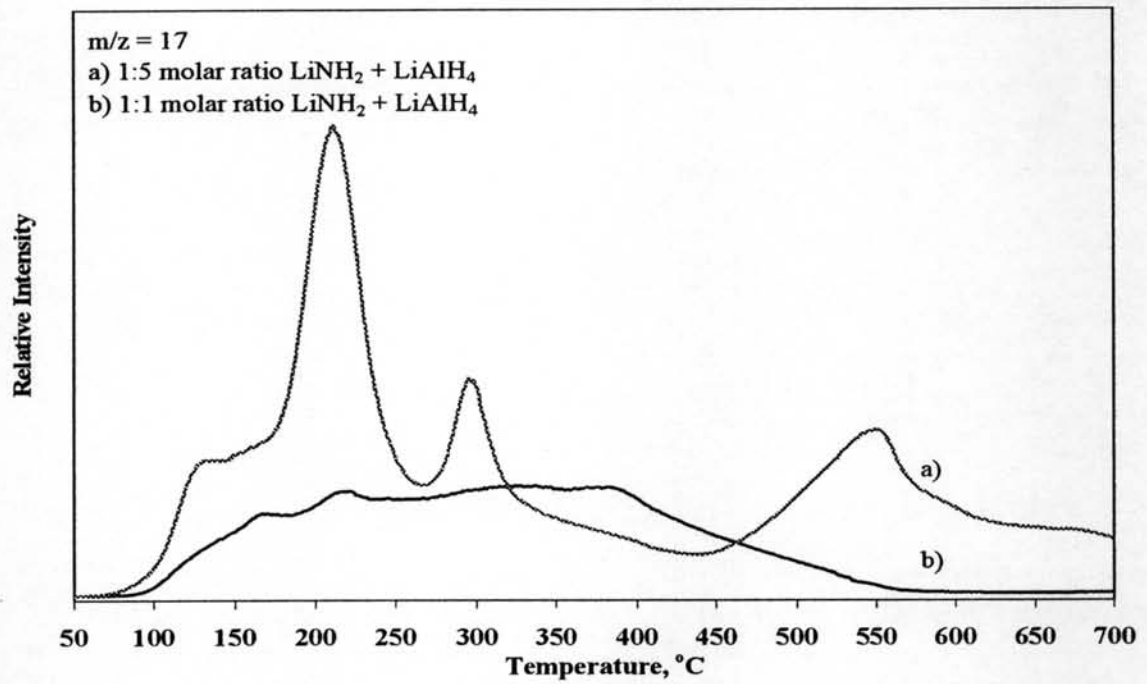

Figure 4.24 TPD-MS patterns of ammonia (m/z = 17) from the mixture of $LiNH_2$ and $LiAlH_4$: a) 1:5 mol ratio and b) 1:1 mol ratio.

Figure 4.25 shows the TPD-MS patterns of a 1:1 mol ratio of $LiNH_2$ and $LiAlH_4$. The main peak of this pattern is ammonia, which desorbs between 100 – 550°C while the hydrogen intensity is much low. The TPD-MS patterns of a 1:5 mol ratio of $LiNH_2$ and $LiAlH_4$ in Figure 4.26 show that the increase in the $LiAlH_4$ loading decreases the ammonia emission and increases the hydrogen intensity. It can be suggested that the higher hydrogen intensity may be from the decomposition of $LiAlH_4$ and the reaction between NH_3 and LiH, which is evidenced by the decrease in the ammonia intensity.

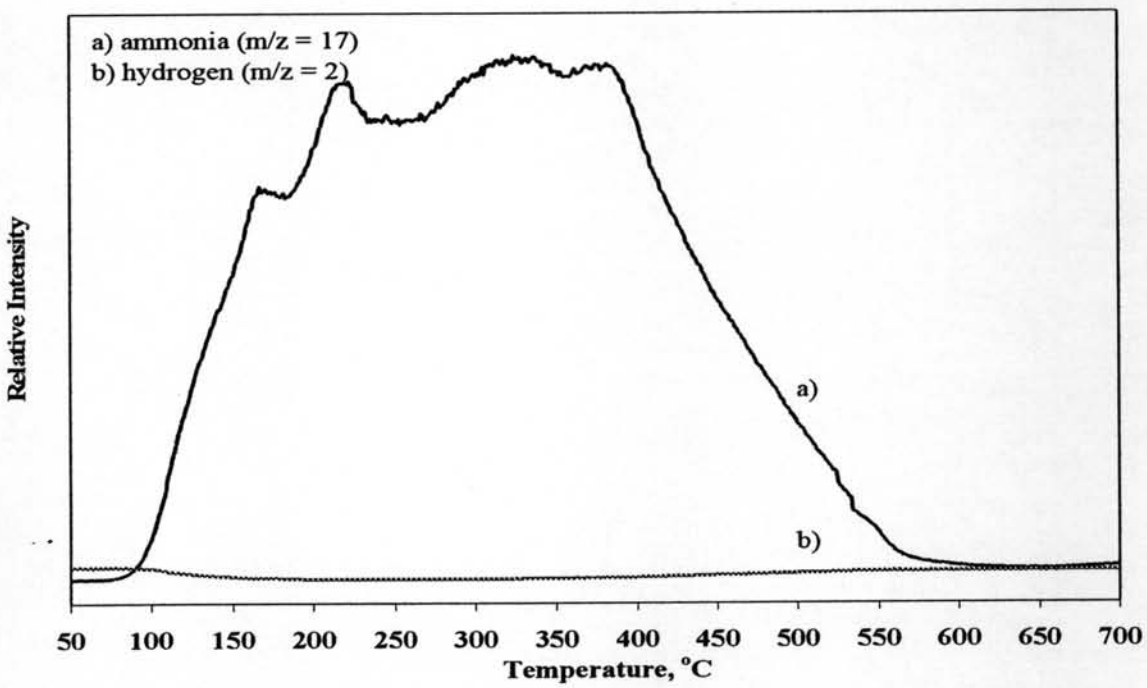

Figure 4.25 TPD-MS patterns from a 1:1 mol ratio of $LiNH_2$ and $LiAlH_4$: a) ammonia and b) hydrogen.

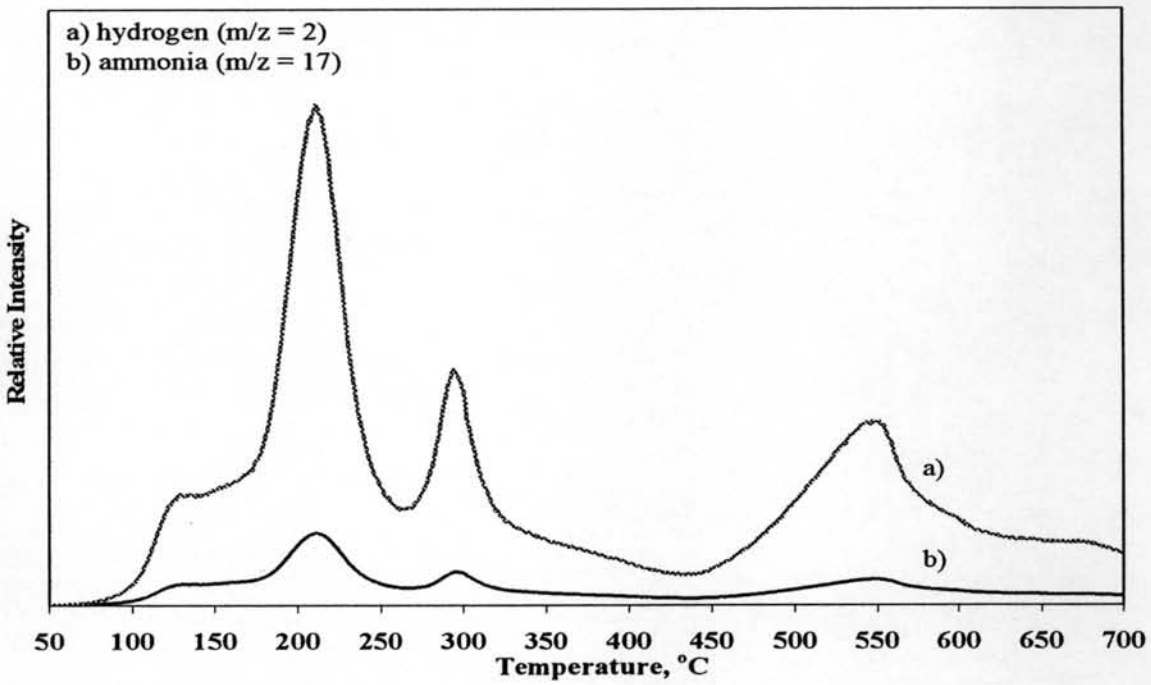

Figure 4.26 TPD-MS patterns from a 1:5 mol ratio of $LiNH_2$ and $LiAlH_4$: a) hydrogen and b) ammonia.

4.5.3 Effect of Catalyst on $LiNH_2/LiAlH_4$

Comparison between a 1:5 mol ratio of $LiNH_2$ and $LiAlH_4$ with and without 4 mol% $ZrCl_4$ is shown in Figure 4.27. It is clearly seen that $ZrCl_4$ decreases ammonia emission. The ammonia and hydrogen intensity of the 1:5 mol ratio of $LiNH_2$ and $LiAlH_4$ doped with 4 mol% $ZrCl_4$ is shown in Figure 4.28. It shows the lower desorption temperature for both ammonia and hydrogen than that of the undoped sample (Figure 4.26). In this case, the catalyst decreases the desorption temperature of the sample.

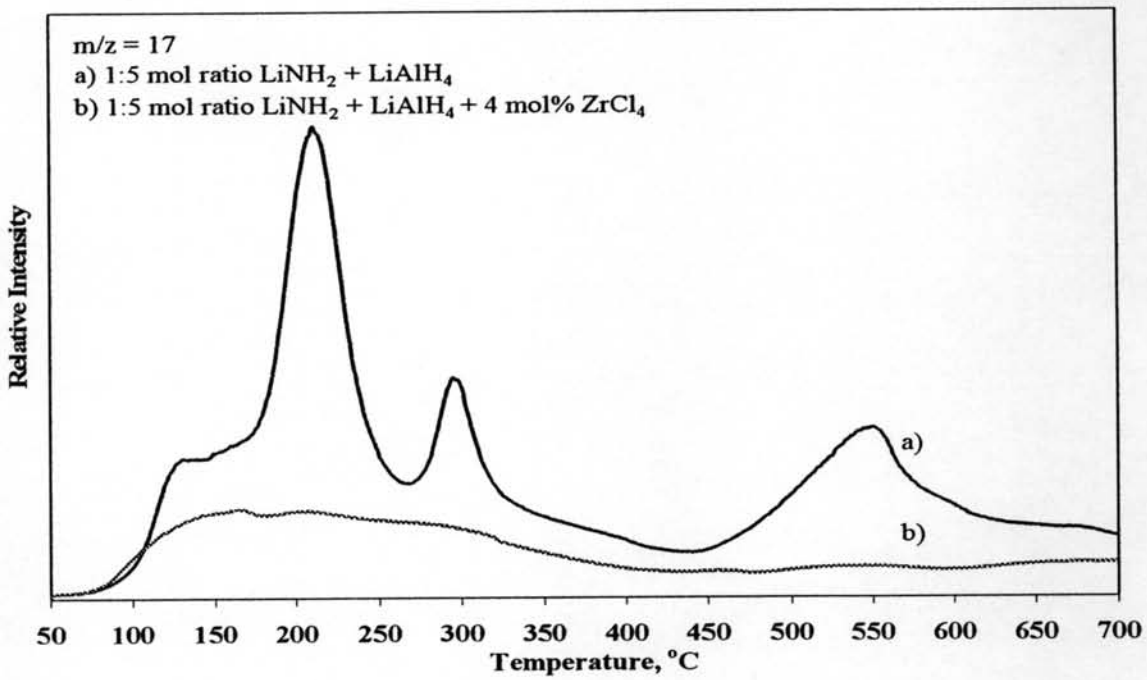

Figure 4.27 TPD-MS patterns of ammonia (m/z = 17) from a 1:5 mol ratio of $LiNH_2$ and $LiAlH_4$ by using agate ball milling for 1 h: a) undoped and b) doped with 4 mol% $ZrCl_4$.

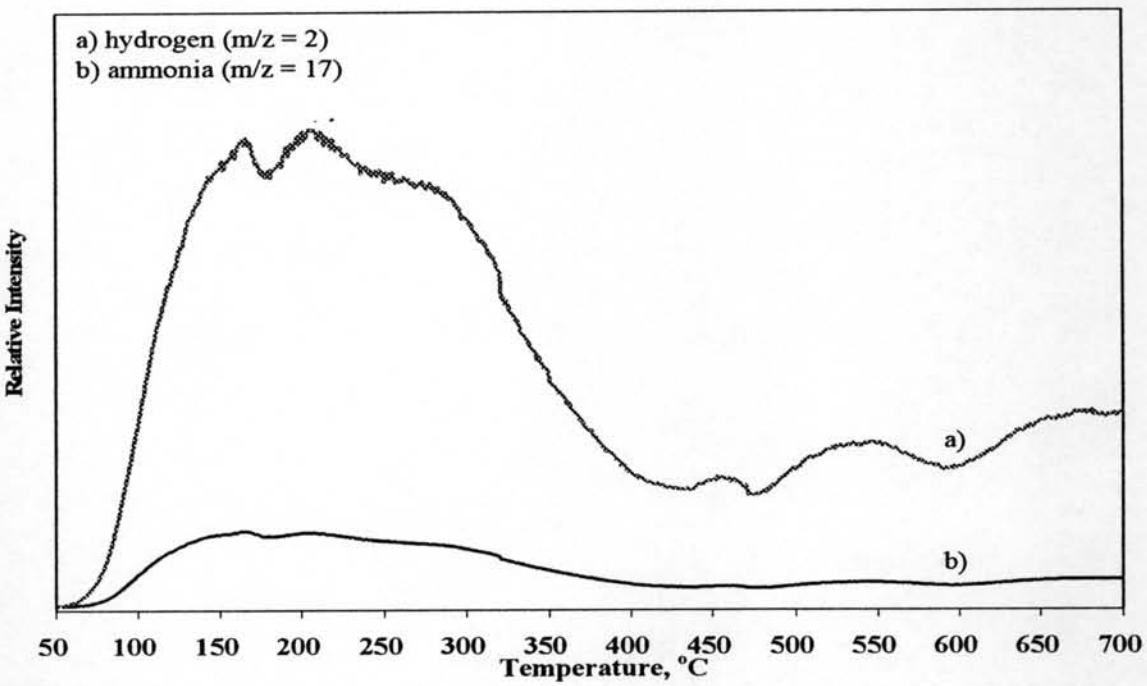

Figure 4.28 TPD-MS patterns from a 1:5 mol ratio of $LiNH_2$ and $LiAlH_4$ doped with 4 mol% $ZrCl_4$ by using agate ball milling for 1 h: a) hydrogen and b) ammonia.

4.5.4 Effect of Two-Layered Packing Sample

To confirm the reaction between ammonia from the decomposition of $LiNH_2$ and LiH from the decomposition of $LiAlH_4$ should have long enough contact time to result in H_2, the two-layered packing sample was studied. Figure 4.29 shows TPD-MS patterns of the two-layered on a 1:5 mol ratio of $LiNH_2$ and $LiAlH_4$, each of which is doped with 4 mol% $ZrCl_4$. The catalyst can decrease the desorption temperature, the highest peak of hydrogen is at 100°C and the two-layered packing can increase the hydrogen desorption.

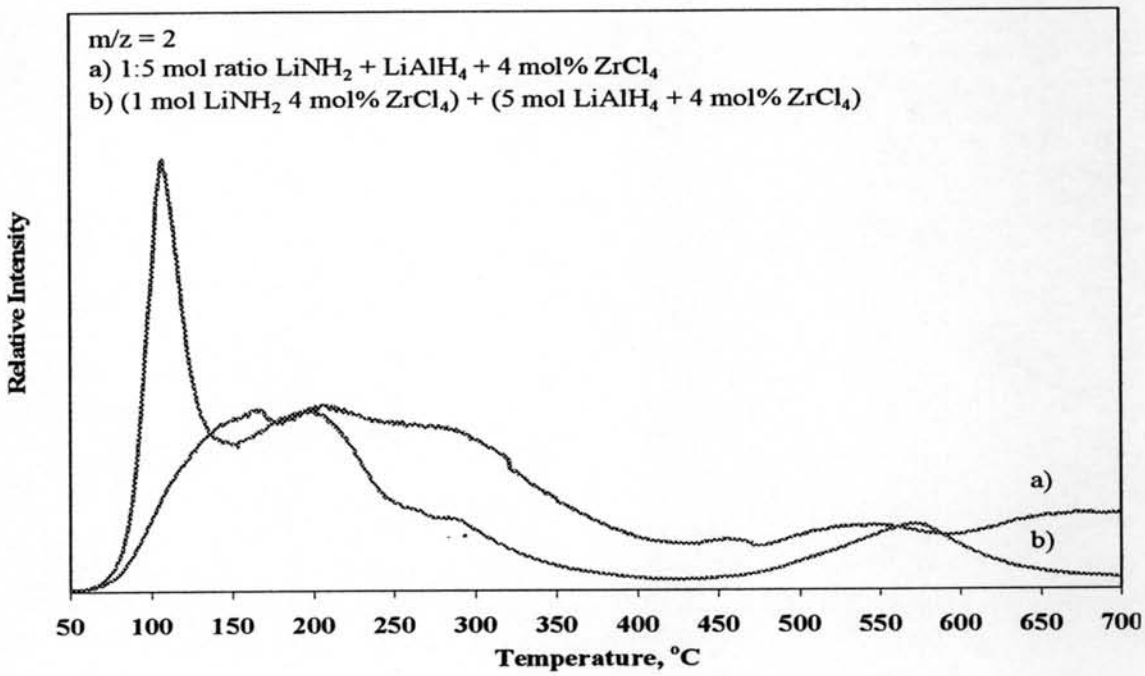

Figure 4.29 TPD-MS patterns of hydrogen (m/z = 2) from a 1:5 mol ratio of $LiNH_2$ and $LiAlH_4$ doped with 4 mol% $ZrCl_4$: a) two-layered sample each of which doped with 4 mol% $ZrCl_4$ and b) one-layered sample.